

UC Berkeley

Working Papers

Title

Individual Vehicle Speed Estimation Using Single Loop Inductive Waveforms

Permalink

<https://escholarship.org/uc/item/2zz4b12p>

Authors

Sun, Carlos
Ritchie, Stephen G.

Publication Date

1999-10-01

CALIFORNIA PATH PROGRAM
INSTITUTE OF TRANSPORTATION STUDIES
UNIVERSITY OF CALIFORNIA, BERKELEY

Individual Vehicle Speed Estimation Using Single Loop Inductive Waveforms

**Carlos Sun,
Stephen G. Ritchie**

**California PATH Working Paper
UCB-ITS-PWP-99-14**

This work was performed as part of the California PATH Program of the University of California, in cooperation with the State of California Business, Transportation, and Housing Agency, Department of Transportation; and the United States Department Transportation, Federal Highway Administration.

The contents of this report reflect the views of the authors who are responsible for the facts and the accuracy of the data presented herein. The contents do not necessarily reflect the official views or policies of the State of California. This report does not constitute a standard, specification, or regulation.

Report for 336

October 1999

ISSN 1055-1417

Individual Vehicle Speed Estimation Using Single Loop Inductive Waveforms

By Carlos Sun¹ and Stephen G. Ritchie², member, ASCE

ABSTRACT: Travel time is the reciprocal of speed and is a useful measure of road congestion and traffic system performance. Travel time is also a basic traffic variable that is used in many Intelligent Transportation System (ITS) strategies such as route guidance, incident detection, and traveler information systems. Previously, speeds were mainly acquired from double inductive loops configured as speed traps, since single loop speed estimates based on assumptions of a constant vehicle length were inaccurate. However, more accurate measurements of speed can now be accomplished with single loops by utilizing inductive waveforms of vehicles that are outputted from newer detector cards. An algorithm using signal processing and statistical methods was developed to extract speeds from inductive waveforms. The results show that the proposed algorithm performs better than conventional single loop estimation methods. The results also show that the algorithm is robust under different traffic conditions and is transferrable across surveillance sites without the need for recalibration. The use of the extensive single loop surveillance infrastructure is a cost-effective way of obtaining more accurate network-wide travel time information.

Key Words: speed estimation, inductive waveform, vehicle signature, single loop detector

¹Assistant Professor, Department of Civil and Environmental Engineering, Rowan University, 201 Mullica Hill Road, Glassboro, New Jersey 08028-1701.

² Professor and Chair, Department of Civil and Environmental Engineering and Institute of Transportation Studies, University of California, Irvine, California 92697-2175.

INTRODUCTION

Speed is a fundamental traffic variable that is applicable to both macroscopic and microscopic analysis. Individual vehicle speed is the distance traveled divided by the time taken to traverse that distance. In other words, speed measures the rate of motion. The averaging of individual vehicle speeds produces the space mean speed variable in the fundamental traffic flow equation (Wardrop, 1952) of

$$q = k v$$

Where:

q = volume

k = density

v = speed

The inverse of speed is travel time which is a very useful performance indicator of the transportation supply system. However, speeds are usually measured at points (over short distances) while travel times are used to indicate the duration of travel over a section of roadway or an entire trip. It is therefore necessary to sample speed at multiple points on a section in order to obtain an accurate estimate of the travel time. If an extensive inductive loop infrastructure exists, then travel times can be estimated accurately even during congested traffic conditions. The collection of accurate vehicle speeds for deriving travel times is therefore critical to government agencies, travellers, and university researchers for applications ranging from real-time traffic control to long term transportation planning.

REVIEW OF SPEED MEASUREMENT METHODS

There is significant ongoing research in the area of traffic surveillance. Old technologies are constantly being refined while new technologies are being developed for use in transportation. Evaluation of different detection technology have been performed at different levels of government. For example, Hughes and JHK & Associates (1994) investigated detection technologies for the United States Department of Transportation and the Federal Highway Administration. On the state level, for example, Bahler et al. (1998) tested non-intrusive traffic detection technologies for Minnesota Department of Transportation. A useful reference on traffic detector technologies is the Traffic Detector Handbook published by the Institute of Transportation Engineers (ITE, 1990). Some technologies that are capable of measuring speed either directly or via post-processing include: inductive loop, piezoelectric, radar, acoustic, ultrasonic, video, and magnetic (Klein, 1995). Even though many new technologies have great potential for future widespread implementation, it is also valuable to improve current detection technology. This is specially relevant to inductive loop detectors, since there is a significant existing infrastructure. For example, in the state of California alone, the California Department of Transportation estimates that there are approximately 300,000 existing inductive loop detectors on California freeways (PATH 1997). This number does not include the significant number of loops deployed in individual cities.

There are two ways of measuring speed using inductive loop detectors. The first way is to use a set of double loops in a speed trap configuration. The speed trap refers to the measurement of the time that a vehicle requires to travel between two detection points (Woods et al., 1994). Woods et al. also discuss other aspects of the speed trap

design including optimum speed trap spacing. Speed is measured as

$$v = \frac{d}{t_{on}^2 - t_{on}^1}$$

Where:

v = speed

d = distance between detectors

t_{on}^1 = time when the first detector turns on

t_{on}^2 = time when the second detector turns on

In addition to the turn on times, the Traffic Control Systems Handbook (Wilshire et al., 1985) recommends the use of turn off times also in order to improve the speed accuracy. The averaging of the turn on and off times results in the following equation:

$$v = \frac{1}{2} \left(\frac{d}{t_{off}^2 - t_{off}^1} + \frac{d}{t_{on}^2 - t_{on}^1} \right)$$

Where:

t_{off}^1 = time when the first detector turns off

t_{off}^2 = time when the second detector turns off

The second way of measuring speed is by using a single loop detector. In other words,

$$v = \frac{l}{t_{off} - t_{on}}$$

Where:

l = effective length, vehicle length + detector length

t_{on} = time when the detector turns on

t_{off} = time when the detector turns off

Since actual vehicle lengths are not known, a mean vehicle length must be assumed for this computation. Because lengths can vary greatly from vehicle to vehicle, the use of a mean vehicle length can result in inaccurate measurements of speed. For example, longer trucks will produce underestimated speeds, and shorter passenger cars will produce overestimated speed.

Another approach of estimating average speed using single loops is by using fundamental traffic flow considerations. The average speed is estimated by using average lane volume and loop occupancy. Some publications that discuss this approach include Athol (1965), Hall et al. (1989), and Jacobson et al. (1989). Speed is expressed in these approaches as

$$v = \frac{q}{o * g}$$

Where:

v = space mean speed

q = flow

o = occupancy

g = factor that takes into account the vehicle and detector length

Hall et al. discusses the use of a sliding value of g which changes with occupancy and is calibrated separately for each set of geometric conditions. This approach assumes that traffic flow is uniform, occupancy is a constant multiple of density, and vehicle lengths are constant. Speed inaccuracies result when the assumed conditions are invalid. Mikhalkin et al. (1972) shows that an estimate using this approach will

produce a biased estimate of the space mean speed. Also, individual vehicle speeds are not estimated with this approach.

In order to produce an unbiased estimate of individual and mean speed using single loops, Mikhalkin et al. (1972) suggests the use of the minimum mean square error estimator for speed. This approach assumes that random vehicle arrival times are uniformly distributed. This approach also necessitates the estimation of the unbiased mean vehicle length during the relevant time interval.

The use of single loop vehicle waveforms for measuring speed has many advantages over previous approaches of speed derivation using loops. First, it can be implemented with existing single loop infrastructure without cutting new loops for speed traps. Second, there is no assumption of a mean vehicle length, so the accuracy of computing speed is not a function of the distribution of vehicle lengths. Third, in contrast to "traffic flow approaches", there is no assumption of traffic uniformity, and individual vehicle speeds in addition to mean speeds can be obtained. Last, there is no distributional assumptions made on vehicle arrival times or vehicle speeds.

The discussion on the use of fundamental traffic flow variables for estimating space mean speed is a critical topic but is out of the scope of this paper. The research in this paper is only concerned with the accurate measurement of individual vehicle speeds by using vehicle waveform analysis.

BACKGROUND

The inductive loop detector is a vehicle surveillance system that is capable of sensing vehicle presence or passage and transmitting the information to the traffic controller. Some references on the operation of the inductive loop detector include Taylor (1972), ITE (1990), and Provenza (1985). The two main components of the inductive loop detector system are the loop system and the detector card. The loop system is a combination of loops of wires connected through transmission lines (lead-ins) to the traffic cabinet. The detector card is an electronic unit that energizes the physical loop with a periodic signal. A magnetic field is induced around the loop by the resonance circuit of the detector card. The sensing of vehicles is accomplished by computing the change in the total inductance of the loop system caused by the vehicle disturbing the loop magnetic field. In the case of some advanced detectors,

this changed in inductance can be recorded at small time intervals. As a result, the inductive waveform of a vehicle can be recorded by sampling the inductance change multiple times.

Figure 1 shows four examples of vehicle inductive waveforms recorded by sampling the detector at short time intervals. The vertical axis represents the relative inductance change and the horizontal axis represents time. A continuous curve is shown instead of the actual discrete curve in order to clearly display the shapes of the waveforms.

The hardware necessary for collecting vehicle waveforms is composed of four different components: the data collection computer, time synchronization source, physical loops, and the detector cards. The data collection process is as follows. After the detector samples the inductance change from the loops, it transmits the inductive waveforms to the data collection computer for storage. An optional Global Positioning System is included in the setup to obtain accurate time stamps. Figure 2 illustrates the hardware interconnect for instrumenting a two lane highway.

METHODOLOGY

As was shown in Figure 1, the vehicle inductive waveforms contain both a leading and a trailing edge. These edges are slew rates which represent the rate of the metallic mass of the vehicle moving over the loop magnetic field. The waveform within these edges is produced when the entire vehicle is covering the loop. This portion of the waveform is no longer the slew rate because of the integration property of the loops, and produces no useful speed information. The estimation of vehicle speed using single inductive loop detectors involves two main procedures. The first is the extraction of the vehicle slew rate or edges from the inductive vehicle waveform. The second is the estimation of the vehicle speed based on the slew rate.

Slew Rate Extraction

There are several steps to extracting the slew rate information from the inductive vehicle waveform. Figure 3a. shows one example of a vehicle waveform that will be used to illustrate the process of slew rate extraction. The y-axis has units of percentage change of inductance counts, and the x-axis has units of milliseconds. Note that the vehicle waveform which results from decreases in inductance have been

inverted to facilitate analysis. The first step in extracting slew rates is to eliminate waveform oscillations that have inductance values near the baseline inductance. This is accomplished by using an arbitrary threshold that will eliminate all oscillations while preserving as much waveform information as possible. A value of 10%-20% was found to be a good threshold from empirical trials with different datasets. The oscillations near the baseline occur because the detector card is constantly trying to adjust the base inductance value in order to compensate for changes in absolute inductance due to environmental and other effects. The oscillations also occur because vehicles are composed of a complex combination of metallic masses including the undercarriage, the engine, and axles. Figure 3b. shows an example of a waveform with the oscillations removed.

The next step is to extract the leading and trailing edges of the vehicle waveform. These edges are slew rates in the sense that they represent the rate of movement of the vehicle's metallic mass over time. The waveform edges in this case have units of % inductance change over time. The upper end of the waveform edges are found by detecting a local maximum point in the vehicle waveform. Therefore the termination point of the waveform edge is defined as

$$f(x) \leq f(c), \forall x \in S$$

Where:

- c = the time at which the local maximum occurs
- $f(c)$ = the local maximum
- $f(x)$ = the value of the waveform or inductance change at a time x
- S = the set of time values that include a single local maximum

Since the waveform is actually a discrete waveform, the termination point of the leading and trailing edges are found by searching for a local maximum by starting from the threshold value that is illustrated in Figure 3b. The resulting leading and trailing edges are shown as solid curves in Figure 3c.

Description of Data

Since different data sets were used in the development of the speed measurement algorithm, the details of the data sets are presented here before the algorithm. The inductive vehicle waveform data was collected on June 30, 1998 in Irvine, California. Figure 4 shows the arterial data collection site in Irvine, California. This site consists

of two detector stations bounding a two lane section of Alton Parkway between the intersections with Telemetry and Jenner streets. Each loop station has double loops for speed measurements. Waveform pairs were collected, since each loop produced one waveform. The distance between the two loop stations is 425 feet. The loops were standard 1.83mX1.83m (6ftX6ft) rectangular loops that are commonly used by many state and city agencies. Video was instrumented on each lane on both the upstream and downstream stations. Video was used to confirm the flow values obtained from the detectors, and to check the road traffic conditions.

There were two data collection periods. The morning peak data was collected between approximately 8:00am and 9:30am at the downstream station. This dataset contained 581 vehicle signature pairs. The average flow over that time period was 612 VPH for two lanes. Due to arterial signalization and varying traffic demand, different speeds, acceleration profiles, and traffic flow levels were observed during the 1-1/2 hour period. The maximum observed speed was 30.66m/s (68.68mph). The minimum speed was 5.47m/s (12.25mph). The arithmetic mean speed was 20.77m/s (46.52mph). The standard deviation of the speed was 4.11m/s. The longest electronic length (length of detector+vehicle) observed was 20.31m. The shortest electronic length observed was 3.89m. The mean electronic length was 4.83m.

The midday data was collected between approximately 12:00pm and 1:00pm at the upstream station. This dataset contained 530 vehicle signature pairs. The average flow over the midday period was 575 VPH. The maximum observed speed was 32.52m/s. The minimum speed was 15.16m/s. The arithmetic mean speed was 22.13m/s. The standard deviation of the speed was 2.61m/s.

Figure 5 shows the percent relative frequency speed distributions for the two datasets. Both the morning and midday datasets contained a wide range of traffic flow conditions and vehicle speeds. This diversity is useful for developing and testing speed computation algorithms. The two datasets are collected from two different sites at different times of the day. Therefore these datasets can be used to test the transferability of the algorithms. Both datasets also contained a wide range of vehicle types including minivans, sports utility vehicles, trucks, buses, and semi-trailer trucks.

Speed Estimation

The first step in the development of the speed computation algorithms is to plot the available data and to analyze the data graphically. Figure 6. confirms our intuition that the slew rate is linearly correlated with speed. The correlation coefficient for the slew rate and speed is 0.8866 for morning peak data and 0.7762 for midday. Furthermore, Figure 6 also shows that a linear relationship exists between the slew rate and the speed. The scatter plots are also used to compare the data from loop 1 and loop 2 at each double loop station. The plots confirm our intuition that each loop in the double loop station produces data with similar correlation between slew rate and speed. The plots of the morning peak downstream using loop 2 and the midday upstream using loop 1 are not shown as they are almost identical to the plots shown in Figure 6.

The next step is to model the relationship between slew rate and speed in order to predict and/or compute speeds. Given the scatter plots shown in Figure 6, the following simple linear model is postulated for the slew rate/speed relationship of the population.

$$speed_i = \alpha + \beta slew_i + \varepsilon_i$$

Where:

- $speed_i$ = dependent variable
- $slew_i$ = independent variable, slew rate
- ε_i = disturbance term

In the context of linear regression,

$$\begin{aligned} sp\hat{e}ed_i &= a + b slew_i \\ e_i &= speed_i - sp\hat{e}ed_i \end{aligned}$$

Where:

- $sp\hat{e}ed_i$ = estimates of the speed

$slew_i$ = regressor, slew rate
 a, b = parameters of regression
 e_i = residual

The following assumptions are made in order to perform linear regression. First, there is the assumption that no observations on $slew_i$ convey information about the expected value of the disturbance. In other words, the conditional expected value of the disturbance is equal to zero. This is a reasonable assumption since only the measurement errors and the random vehicle fluctuations contribute to the disturbance. The random vehicle fluctuations are the result of different driving behavior and vehicle mechanics. Second, the assumption of homoscedasticity is made. Last, the disturbances of the slew rates are assumed to be uncorrelated. The last two assumptions are also reasonable since there is nothing in the loop resonant circuit theory to suggest that variance is not constant across slew rates and that disturbances are correlated. These assumptions are supported by residual tests, and test outcomes are reported in the results section.

Least square estimation, which tries to minimize the sum of square residuals, is used to determine the parameters a and b . The solution of the following normal equations yields the parameters of the regression model.

$$\begin{aligned}
 a n + b \sum_{j=1}^n slew_j &= \sum_{j=1}^n speed_j \\
 a \sum_{j=1}^n slew_j + b \sum_{j=1}^n slew_j^2 &= \sum_{j=1}^n slew_j speed_j
 \end{aligned}$$

Speed can then be predicted or computed for a vehicle by using the linear regression model and a given slew rate for that vehicle.

An interesting experimental concern arises when the standard error of b is examined in the following equation (Wannocott, 1990):

$$standard\ error \approx \frac{\sigma}{\sqrt{n}} \cdot \frac{1}{S_{slew}}$$

The above equation implies that by increasing S_{slew} , the standard error of b can be reduced. This suggests that one might want to collect the regression data by driving control vehicles over the loops with as wide a spread of slew rates as possible. However, this approach is a costly approach that detracts from the ease of implementation of the proposed speed computation system. Consequently, only data from natural occurring traffic is used for calibrating the proposed system.

Derivation of Ground Truth

The ground truth for individual vehicle speed is derived by using double loop data. Both digital and analog detector outputs were obtained during the vehicle waveform data collection. Double loop speeds that are computed using digital outputs can have typical errors of between 3% and 5% for commonly observed vehicles such as cars and pickups (Woods et al. 1994).

Pusula et al. (1989) found that the standard error of the speeds measured with analog waveforms is only one third of the error of the speeds with the traditional digital output from thresholds. The measurement of vehicle speed is determined by using the 50% amplitude point of the leading edge of the waveforms from loop 1 and 2 (Pusula et al. 1994). Thus, this technique is used in deriving the ground truth.

Figure 7 illustrates the double loop speed computation process. In this figure, the first waveform corresponds to the first loop in the speed trap, and second waveform corresponds to the second loop. For each waveform, the front edge is linearized, and the 50% point is determined and shown as a circle in the figure. The vehicle travel time is the difference between the time corresponding to the first circle and the second circle. Since the distance between the double loops is known, the speed is determined by dividing this distance by the travel time.

An alternate method that requires less computation is to use the peak of the waveforms. Waveform peaks are shown as asterisks in Figure 7. This method is less accurate since a waveform can have a plateau instead of a single peak. In fact, the example in Figure 7 exhibits such inaccuracies.

Regardless of which double loop speed computation method is used, there is some error associated with the measured speeds. More precise instrumentation composed of infrared beam curtains or high precision Doppler radars could yield a more accurate ground truth, but the cost of these devices prohibited their use for this

research. Therefore the inaccuracy of the ground truth could have contributed to the error in the research results.

RESULTS

First the results from the linear regression will be shown. Then comparisons will be made with other single loop estimation methods. The sensitivity of the regression parameter with respect to the calibration size will be analyzed, and other model form possibilities will be discussed. In the results section, the term calibration is used to describe the process of estimating regression parameters.

The downstream morning peak dataset was divided into 300 vehicles for calibration, and the remaining 281 for testing. Linear regression was performed by using the first 300 vehicle waveforms from the second loop only, so an additional 300 vehicle waveforms from the first loop are also available for testing. The regression coefficient as well as several measures that are commonly included in regression analysis are listed in Table 1. The t-statistic shows that all coefficients are significant. The R^2 value confirms that a large fraction of the variance of the speed can be explained by the slew rate. The standard error shows that about two-thirds of the residuals will lie between -1.90m/s and +1.90m/s. The large value for the slope is due to the fact that the units of the independent variable is in term of % inductance change per millisecond.

Some analysis was performed on the regression residuals in order to validate the normality assumptions of the error term (ϵ) and to verify that the error terms are not correlated. The error term is assumed to be distributed $N(0, \sigma_\epsilon^2)$, which means that it is normally distributed with zero mean and constant variance. Figure 8 shows the histogram of the residuals along with the table of descriptive statistics. The histogram and the statistics both show that the distribution of the residuals do not deviate significantly from normal, and the expected value of the distribution is almost zero. In order to test for heteroscedasticity, hypothesis testing is performed using the following null and alternate hypotheses:

$$H_0: \sigma_i^2 = \sigma^2, \forall i$$

$$H_1: \text{any } \sigma_i^2 \neq \sigma^2$$

The application of White's heteroscedasticity test (White 1980) produced a small F-value of 0.6172, which means the null hypothesis cannot be rejected and the errors are homoscedastic. The Durbin-Watson statistic was 1.655 which shows only small evidence for autocorrelation, thus the model is not adjusted for time-ordered effects.

Table 2 shows the results comparing three different single loop speed computation methods. The test data is composed of 281 vehicles from the downstream morning peak data. The first column, labeled waveform speed, is the speed computed by the approach of using inductive waveform slew rates. The second column, labeled unbiased speed, is the speed computed in the conventional fashion by using an unbiased estimate of the mean effective length (length of vehicle and detector). The estimated effective length was found to be 4.83 meters for the downstream morning dataset. This length is divided by the loop traversal time of the vehicle to obtain unbiased individual vehicle speed. The third column, labeled biased speed, is the speed computed by using a commonly assumed effective length of 6.55m (21.5ft) (Arendonk, 1996). An assumed effective length is commonly used by transportation agencies, since it does not require the sampling of vehicle lengths for estimating a sample mean. The data from the second loop of the speed trap is used for testing all three speed computations.

The results from Table 2 show that the waveform speed algorithm performed better than other conventional speed computation methods. The waveform speed was more accurate and shows less variability than the other two approaches. A value of 8.7% standard deviation for the unbiased speed computation error is not surprising, since this standard deviation is a function of the distribution of vehicle lengths. In locations where the traffic is more homogeneous in term of vehicle type for all times of the day, the unbiased speeds is expected to be much more accurate and to exhibit less variability than the results from Table 2. The biased speed shows a significant average error of 36.9%, since a biased effective length is assumed. This result shows that if an effective length which does not reflect the traffic characteristics of the particular location is assumed, then significant speed computation error will result.

In order to test the transferability of the calibrated algorithm and regression coefficient, speeds are recalculated using the vehicle waveforms from the first loop instead of the second loop. In other words, the second loop waveforms are used for calibration, while the first loop waveforms are used for testing. The results in Table 3 show the average error and the standard deviation of error increased only slightly

when using testing data. Table 3 presents some evidence for the transferability of the calibrated algorithm.

In order to further verify the transferability of the calibrated algorithm, testing is performed using the vehicle waveforms from a different location recorded at a different time of the day. This dataset is recorded at the upstream site during midday. The results in Table 4 reaffirms the robustness of the algorithm. The average error remained the same while the standard deviation of error increased only slightly. It is interesting to note that the unbiased speed, computed using the unbiased mean effective length of this dataset, shows less error than the morning dataset. This result reflects the more homogeneous midday traffic that contains less truck traffic and more lunch time passenger vehicles.

The sensitivity of the regression parameter with respect to the calibration size and the associated average estimation errors are shown in Figure 9. Figure 9a. shows that the regression slope fluctuates when less data is used for calibration, but the value levels off after 300 vehicles are used. This is the reason for using a calibration dataset size of 300 vehicles. Figure 9b. shows the sensitivity of the average prediction error using a test data size of 231 vehicles. In terms of average prediction error, errors of around 7% are obtained after the calibration size is larger than 25 vehicles. However, regression theory shows that a larger variability in the independent variable leads to smaller standard errors in the residuals; therefore, a more conservative calibration size such as 300 vehicles will most likely contain more variability. Regression can also be accomplished by selecting a small set of vehicles that have a wide range of speeds, but such a set is not contiguous in terms of arrival times and does not lead to real-time calibration.

Table 5 shows the regression results of using other models forms to describe the relationship between slew rate and speed. The t-statistic show that some coefficients of these more complicated model forms were not statistically significant. The R^2 values and the standard errors of regression are all similar between these model forms and the linear model. Also Figure 6 presents a strong graphical evidence for the use of linear regression. Therefore the simpler linear model is adequate for predicting vehicle speeds.

CONCLUSION

This paper presents a new methodology for computing vehicle speeds using single loops. The inductive waveform slew rates are extracted, and a linear regression model is used for deriving speeds from slew rates. Data collected from Irvine, California, shows that this method can perform better than other methods of computing speed. One main advantage this method has over other methods is the fact that the accuracy of predicting speeds is not a function of the distribution of vehicle lengths. Another advantage, is the robustness of the method which is shown to be temporally and spatially transferable. This method requires very little computing power and cost to implement. The simplicity of the methodology leads to uncomplicated real-time implementations for traffic management and control purposes.

The utilization of the current single loop infrastructure avoids costly road closures and equipment associated with the cutting of double loops. In many cities and states, this infrastructure is extensive and can produce speed information for different Intelligent Transportation System needs. However, double loops or other detection systems are still necessary if high accuracy in speed computation is required.

Local accelerations can be computed by using this method if double loops are available. The local accelerations are simply the difference between the speed computed from the first and second loops in a speed trap. The local accelerations can be a valuable input for congestion monitoring and incident detection algorithms. No acceleration results were presented because there was no ground truth available for validating results.

ACKNOWLEDGMENT AND DISCLAIMER

The research reported in this paper was supported by the California Department of Transportation (Caltrans) PATH (Partners for the Advanced Transit and Highways). The contents of this paper reflect the views of the authors who are responsible for the facts and the accuracy of the data presented herein. The contents do not necessarily reflect the official views or policies of the State of California. This paper does not constitute a standard, specification, or regulation.

The authors would like to thank Mr. Joe Palen from Caltrans and Dr. Reinhart Kühne from the University of Stuttgart for their ideas and support. The authors would also like to thank Gardner Transportation Systems for assisting in the data collection.

REFERENCES

- Athol, P. (1965) "Interdependence of Certain Operational Characteristics Within a Moving Traffic Stream." Highway Research Record 72. Pg. 58-87. HRB. National Research Council. Washington, D.C.
- Arendonk, J. (1996) "A Comparison of Real-Time Freeway Speed Estimation Using Loop Detectors and AVI Technologies.", Southwest Region University Transportation Center. Compendium: Graduate Student Papers on Advanced Surface Transportation Systems. Texas Transportation Institute. Texas A&M, College Station. Pg. J1-J40.
- Bahler, S.J., Minge, E.D., and Kranig, J.M. (1998) " Field Test of Non-Intrusive Traffic Detection Technologies." Preprint. Transportation Research Board 77th Annual Meeting. January 11-15. Washington, D.C.
- Hall, F.L., and Persaud, B.N. (1989) "Evaluation of Speed Estimation Made with Single-Detector Data from Freeway Traffic Management Systems." Transportation Research Record 1232. Pg. 9-16.
- Hughes Aircraft Company and JHK & Associates. (1994) "Vehicle Detector Field Test Specifications and Field Test Plan." Task 4 Report for Detector Technology for IVHS. United States Department of Transportation. Federal Highway Administration. Washington, D.C. Contract Number DTFH61-91-C-00076.
- Institute of Transportation Engineers. (1990) Traffic Detector Handbook. Washington, D.C.
- Jacobson, L.N., Nihan, N.L., and Bender, J.D. (1990) "Detecting Erroneous Loop Detector Data in a Freeway Traffic Management System." Preprint. Transportation Research Board 69th Annual Meeting. January 7-11. Washington, D.C.
- Klein, L. (1995) "Modern Detector Technology for Traffic Management." Presentation for the University of California, Irvine. February 28.
- Mikhalkin, B., Payne, H.J., and Isaksen, L. (1972) "Estimation of Speed from Presence Detectors." Highway Research Record 388. Pg. 73-83. HRB. National Research Council. Washington, D.C.
- PATH (Partners for Advanced Transit and Highways) (1997) "Workshop on Research, Development, and Testing of Traffic Surveillance Technologies." Richmond Field Station. California.
- Provenza, J. (1985) "Loop Detector Systems." International Municipal Signal Association Journal, Volume XXII, March-April, Number 2, Pg. 5-7.
- Pursula, M. and Kosonen, I. (1989) "Microprocessor and PC-based Vehicle

- Classification Equipments Using Induction Loops." Proceedings of the Second International Conference on Road Traffic Monitoring. IEE Publication Number 299. London. February 7-9. Pg. 24-28.
- Pursula, M. and Pikkarainen, P. (1994) "A Neural Network Approach to Vehicle Classification with Double Induction Loops." Proceedings, 17th Australian Road Research Board Conference. Part 4. Pg. 29-44.
- Taylor, S.S. (1972) "Inductive Loop Detector Functions." Department of Traffic, City of Los Angeles. Staff Report No. 53.08. February 4.
- Wannacott, T.H. and Wannacott, R.J. (1990) Introductory Statistics. Wiley & Sons. New York.
- Wardrop, J.G. (1952) "Some Theoretical Aspects of Road Traffic Research." Proceedings Instn. Div. Engrs., Vol. 1, No. 2. Pg. 325.
- White, H. (1980) "A Heteroscedasticity-Consistent Covariance Matrix Estimator and a Direct Test for Heteroscedasticity." *Econometrica*, 48, pp. 817-838.
- Wilshire, R., Black, R., Grochoske R., and Higinbotham, J. (1985) Traffic Control Systems Handbook. Institute of Transportation Engineers. Washington, D.C. Report No. FHWA-IP-85-12. April.
- Woods, D.L., Cronin, B.P., and Hamm, R.A. (1994) "Speed Measurement with Inductance Loop Speed Traps." Texas Transportation Institute. Research Report FHWA/TX-95/1392-8. Texas A&M. College Station.

TABLE 1. Linear Regression Results

Output (1)	Coefficient (2)	Standard Error (3)	t-Statistic (4)
a (intercept)	3.597205	0.461335	7.797389
b (slope)	1739.639	46.04257	37.78327
R^2	0.8273		
Standard Error of regression	1.9028 m/s		

TABLE 2. Single Loop Speed Computation Results Using AM Downstream Data

Errors (1)	Waveform Speed (2)	Unbiased Speed (3)	Biased Speed (4)
Average Error (%)	6.7	12.7	36.9
Standard Deviation of Error (%)	5.3	8.7	11.8

TABLE 3. Testing Transferability Using AM Downstream Data

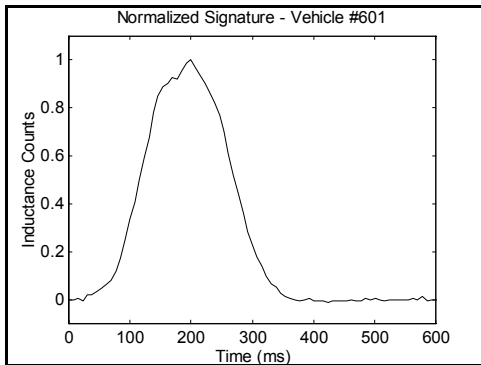
Errors (1)	Waveform Speed Using Second Loop (calibrated) (1)	Waveform Speed Using First Loop (uncalibrated) (2)
Average Error (%)	6.7	7.2
Standard Deviation of Error (%)	5.3	5.9

TABLE 4. Single Loop Speed Computation Results Using Midday Upstream Data

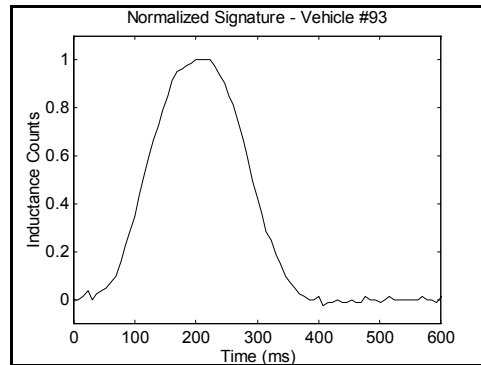
Errors (1)	Waveform Speed (2)	Unbiased Speed (3)	Biased Speed (4)
Average Error (%)	6.7	7.24	37.1
Standard Deviation of Error (%)	5.7	11.73	15.9

TABLE 5. Regression Using Other Model Forms

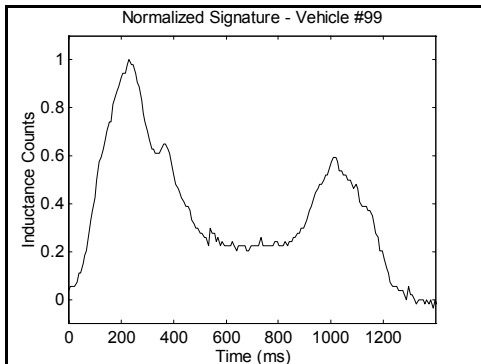
Output (1)	Coefficient (2)	Standard Error (3)	t-Statistic (4)
(a) Quadratic Model Form: $\text{speed} = a + b \text{ slew} + c \text{ slew}^2$			
a	-1.838342	1.016288	-1.808879
b	3028.725	221.9280	13.64733
c	-70812.11	11953.21	-5.924108
R ²	0.845554		
Standard Error of regression	1.802480 m/s		
(b) Cubic Model Form: $\text{speed} = a + b \text{ slew} + c \text{ slew}^2 + d \text{ slew}^3$			
a	-2.564159	2.046421	-1.252997
b	3327.396	783.6314	4.357333
c	-106996.3	89315.42	-1.19960
d	1343666	3286728	0.408816
R ²	0.84541		
Standard Error of regression	1.805012 m/s		



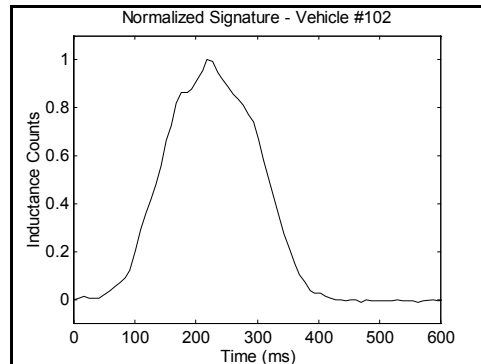
(a)



(b)



(c)



(d)

FIG. 1. Examples of Vehicle Inductive Waveforms: (a) Passenger Car; (b) Sport Utility Vehicle; (c) Semi-Trailer Truck; (d) Minivan

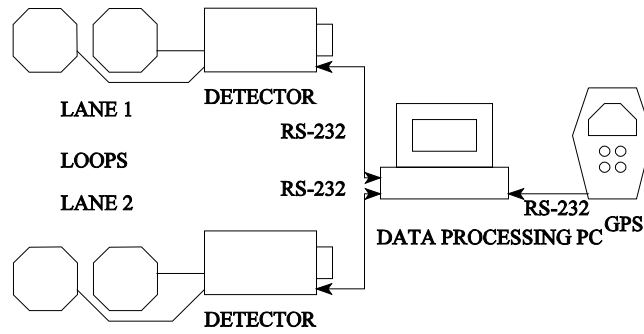
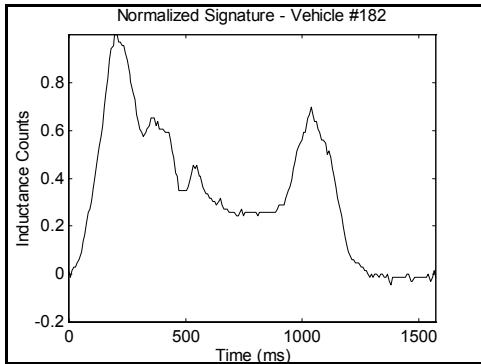
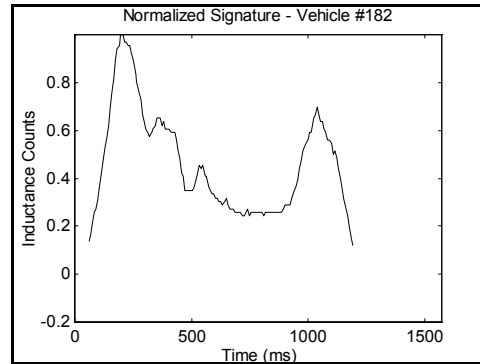


FIG. 2. Waveform Collection Hardware



(a)



(b)

(c)

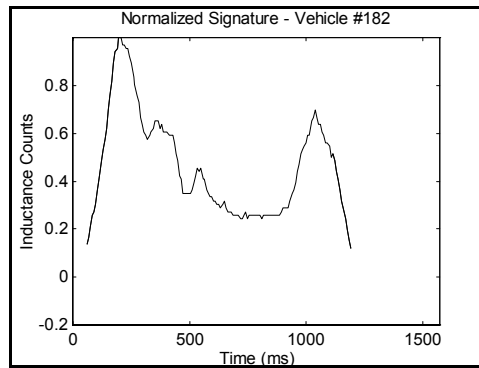


FIG. 3. Slew Rate Extraction Process: (a) Sample Vehicle Waveform; (b) Removal of Base Oscillations; (c) Leading and Trailing Edge Slew Rates

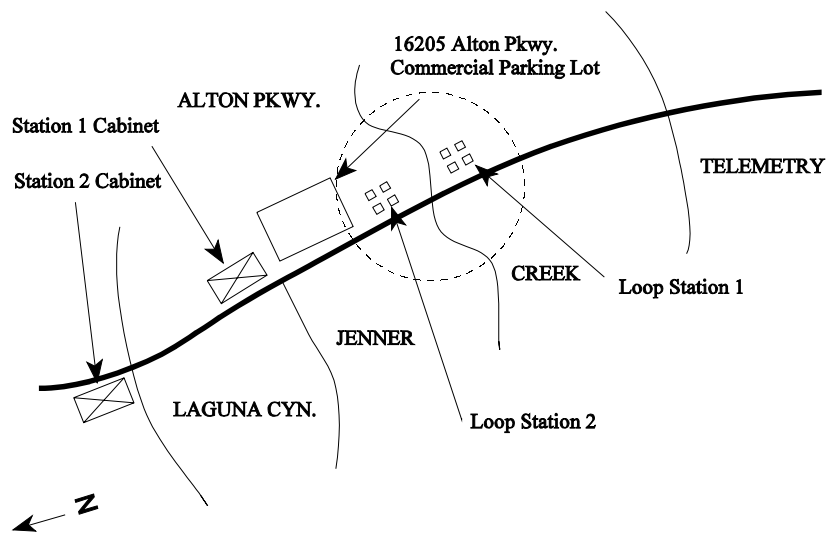
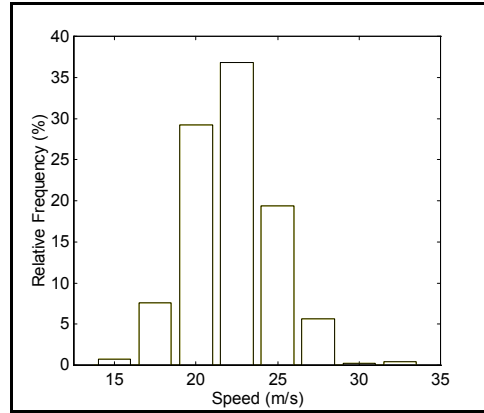
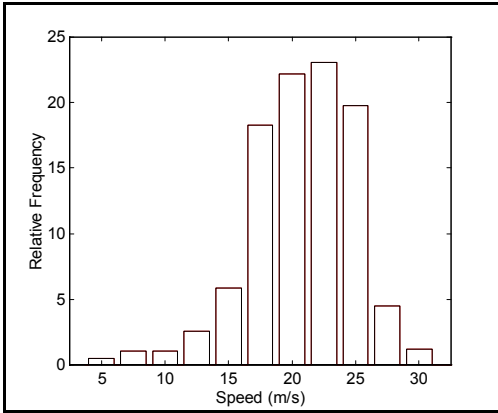
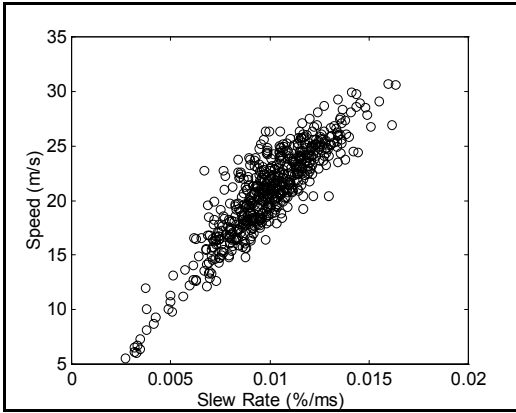


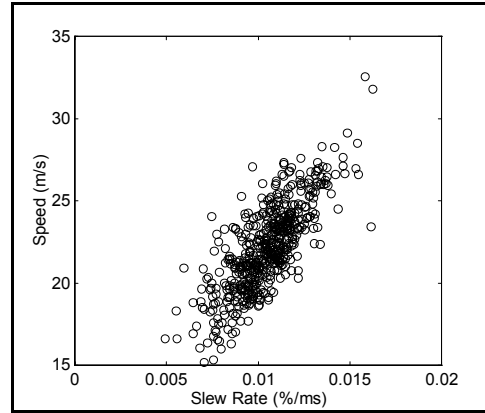
FIG. 4. Data Collection Site



(a) (b)
 FIG. 5. Speed Distributions (Percent Relative Frequency): (a) AM Peak Downstream;
 (b) Midday Upstream



(a)



(b)

FIG. 6. Scatter Plot of Slew Rate and Speed: (a) AM Peak Downstream Using Loop 1; (b) Midday Upstream Using Loop 2

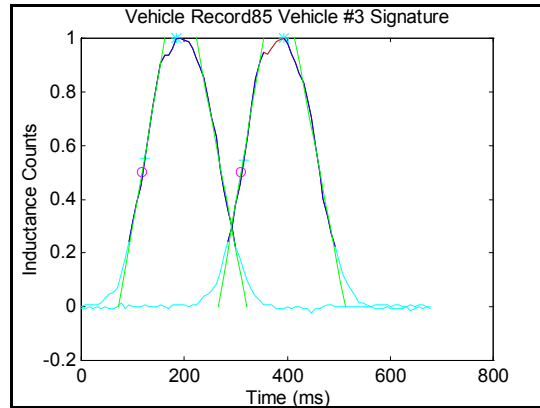


FIG. 7. Double Loop Speed Computation Using Waveforms

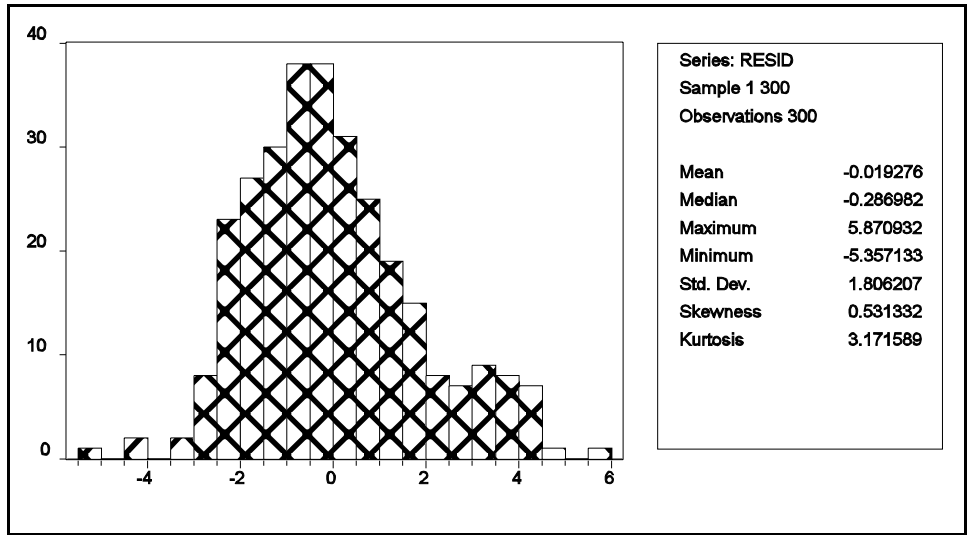
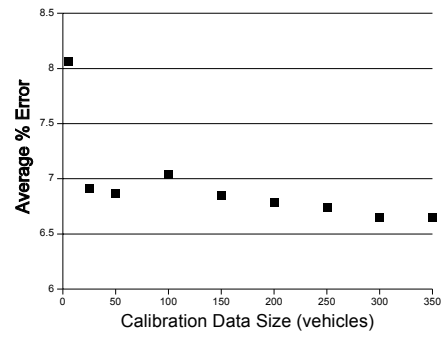
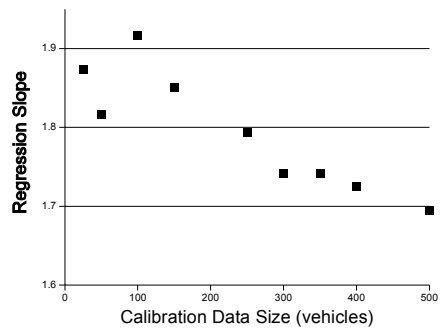


FIG. 8. Regression Residual Analysis



(a) (b)
 FIG. 9. Sensitivity to Calibration Data Size: (a) Sensitivity of Regression Parameters;
 (b) Sensitivity of Average Prediction Error

FIGURE CAPTIONS

FIG. 1. Examples of Vehicle Inductive Waveforms: (a) Passenger Car; (b) Sport Utility Vehicle; (c) Semi-Trailer Truck; (d) Minivan

FIG. 2. Waveform Collection Hardware

FIG. 3. Slew Rate Extraction Process: (a) Sample Vehicle Waveform; (b) Removal of Base Oscillations; (c) Leading and Trailing Edge Slew Rates

FIG. 4. Data Collection Site

FIG. 5. Speed Distributions (Percent Relative Frequency): (a) AM Peak Downstream; (b) Midday Upstream

FIG. 6. Scatter Plot of Slew Rate and Speed: (a) AM Peak Downstream Using Loop 1; (b) Midday Upstream Using Loop 2

FIG. 7. Double Loop Speed Computation Using Waveforms

FIG. 8. Regression Residual Analysis

FIG. 9. Sensitivity to Calibration Data Size: (a) Sensitivity of Regression Parameters; (b) Sensitivity of Average Prediction Error